



Teze disertace
k získání vědeckého titulu "doktor věd"
ve skupině věd technické

Nanoindentation assisted characterization of heterogeneous structural materials

Komise pro obhajoby doktorských disertací v oboru: Mechanika pevných těles

Jméno uchazeče: doc. Ing. Jiří Němeček, Ph.D.

Pracoviště uchazeče: ČVUT v Praze, Fakulta stavební

Místo a datum: Praha, 1. listopadu 2018

Contents

1	Introduction	3
2	Summary	5
3	Principles of nanoindentation	6
4	Highligths of cementitious materials, alternative binders and their microstructure	8
5	Elastic properties and creep effects in cementitious materials	11
6	Nanoindentation on heterogeneous microstructures	14
7	Interfacial transitional zones	18
8	Plasticity, visco-elastic properties and dynamic nanoindentation	19
9	Strength properties	24
10	Conclusions and outlook	30
11	Acknowledgements	31
12	References	32
13	Resume of Jiří Němeček	38

1 Introduction

The dissertation is based on a set of articles of the applicant on nanoindentation of heterogeneous composites. The papers demonstrate research progress done in the area and include some important novelties that were achieved by the applicant and co-workers. For the sake of clarity and overview, the articles are itemized here chronologically as published and with the main achievements reached.

[1]. J. Němeček, Creep effects in nanoindentation of hydrated phases of cement pastes, *Materials Characterization*, vol. 60, pp. 1028-1034, 2009.

Here, the **effect of creep** on evaluation of intrinsic elastic properties on cement was firstly recognized and **artificial source of size effect** on hydrated cement paste was diagnosed.

[2]. J. Němeček, V. Šmilauer, and L. Kopecký, Nanoindentation characteristics of alkali activated aluminosilicate materials, *Cement and Concrete Composites*, vol. 33, no. 2, pp. 163 - 170, 2011.

Here, a specific **deconvolution procedure** with assured convergence in statistical indentation was developed. Also, the work conducted in [2] revealed, for the first time, intrinsic mechanical properties of **N-A-S-H gels** that form a binder phase of alkali-activated aluminosilicate materials, sometimes called geopolymers.

[3]. J. Menčík, L. H. He, and J. Němeček, Characterization of viscoelastic-plastic properties of solid polymers by instrumented indentation, *Polymer Testing*, vol. 30, no. 1, pp. 101 - 109, 2011.

Here, information obtainable from nanoindentation tests on **polymer samples** such as apparent modulus, hardness and components of creep compliance function are described.

[4]. J. Němeček, V. Králík, and J. Vondřejc, Micromechanical analysis of heterogeneous structural materials, *Cement and Concrete Composites*, vol. 36, no. 0, pp. 85 - 92, 2013.

Here, the **statistical grid indentation** was used for identification of various heterogeneous structural materials including **cement paste, gypsum and aluminium alloy**. A mathematically ill-posed problem of deconvolution into infinite number of phases was solved by a priori determination of finite phase number by combining information gained from sample chemistry and SEM. Effective stiffness matrix calculated from averaged stresses and strains in the domain by analytical or FFT-based methods were evaluated.

[5]. W. da Silva, J. Němeček, and P. Štemberk, Methodology for nanoindentation assisted prediction of macroscale elastic properties of high performance cementitious com-

posites,” *Cement and Concrete Composites*, vol. 45, pp. 57 - 68, 2014.

Here, the application of deconvolution and homogenization was successfully used for solving problems on several length scales of materials with even more complex microstructures, the **high-strength cementitious composites**.

[6]. V. Králík and J. Němeček, Comparison of nanoindentation techniques for local mechanical quantification of aluminium alloy, *Materials Science and Engineering: A*, vol. 618, pp. 118 - 128, 2014.

Identification of stress-strain relations, approaches of statical and dynamic indentation were applied to fine **aluminium foam** cell wall here and the published results served later as inputs for a multi-scale FE model [7].

[7]. J. Němeček, F. Denk, and P. Zlámal, Numerical modeling of aluminium foam on two scales,” *Applied Mathematics and Computation*, vol. 267, pp. 506 - 516, 2015.

Approaches of statistical indentation, analytical and numerical **homogenization** on different scales of the metal foam were combined and employed here.

[8]. V. Nežerka, J. Němeček, Z. Sližkova, and P. Tesárek, Investigation of crushed brick matrix interface in lime-based ancient mortar by microscopy and nanoindentation, *Cement and Concrete Composites*, vol. 55, pp. 122 - 128, 2015.

Here, nanoindentation was employed for investigation of the **interface** between lime-based matrix and brick fragments. Evolution of elastic modulus in ITZ combined with SEM-EDS analysis gave unique values used later as input values of a hierarchical multi-scale model of composite strength (Nežerka et al., 2017).

[9]. J. Němeček, V. Hrbek, L. Polívka, and A. Jäger, Combined investigation of low-scale fracture in hydrated cement and metal alloys assessed by nanoindentation and FIB,” in 9th International Conference on Fracture Mechanics of Concrete and Concrete Structures FraMCoS-9, V. Saouma, J. Bolander and E. Landis (Eds), pp. 11-14, 2016.

Here, the first approaches utilizing nanoindentation to assess **cement toughness** from fracture around indents and combining information gained from an indenter and from **FIB sectioning** were published.

[10]. J. Němeček, V. Králík, V. Šmilauer, L. Polívka, and A. Jäger, Tensile strength of hydrated cement paste phases assessed by micro-bending tests and nanoindentation, *Cement and Concrete Composites*, vol. 73, pp. 164 - 173, 2016.

Here, an approach which used direct measurement of microbeams loaded in bending with the aid of nanoindenter gave pioneering results of both **tensile strength** (260-700 MPa) and supremum **fracture energy** (4-20 J/m²) of individual constituents of cement paste. The results of strength and fracture energy of C-S-H gels and calcium hydroxide were

experimentally determined for the first time.

[11]. J. Němeček, V. Šmilauer, J. Němeček, F. Kolařík, and J. Maňák, Fracture properties of cement hydrates determined from microbending tests and multiscale modeling, in Computational Modelling of Concrete Structures: Proceedings of the Conference on Computational Modelling of Concrete and Concrete Structures (EURO-C 2018), February 26 - March 1, 2018, Bad Hofgastein, Austria, Guenther Meschke, Bernhard Pichler, Jan G. Rots (Eds), pp. 113-119, Taylor and Francis Group, London, 2018.

Here, the results obtained in [10] were used in the **multi-scale model** of fracture strength on the C-S-H level of the composite. The cohesive **strength of C-S-H globule** of 2500 MPa was predicted consistently with other (molecular dynamics) simulations found in the literature.

2 Summary

The thesis is focused on nanoindentation applied to various heterogeneous structural composites based mainly on cement or alternative binders. A few examples of specific metal composites (metal foam) and a polymer is solved. Although nanoindentation was historically applied to homogeneous-like materials as finely grained metals, glass, ceramic and polymeric coatings, it has begun a standard micromechanical tool for many other composites. The thesis is written in a chronological manner as a guide that leads the reader through the main microstructural features of the composites and shows characteristics that could not be assessed without the aid of nanoindentation. Firstly, introduction to the specific features of cementitious composites and composites based on alternative binders is summarized in Section 3 and 4. Although many microstructural characteristics were gained through microscopy and chemical analyses in the past, micromechanical characterization of individual microscale components started just recently, about twenty years ago. Naturally, investigations came up with elastic properties whose extraction surprisingly faced significant obstacles in the form of theoretical and physical uncertainties. As one source of errors, creep was identified to have an influence on evaluation of elastic properties. The topic is solved in Section 5).

Intrinsic heterogeneity of cement based composites caused many troubles with micromechanical identification of individual microstructural phases and special approaches combining morphological and elemental analyses with blind indentation needed to be developed. Statistical grid nanoindentation made possible to identify many basic building blocks of structural composites including C-S-H gels in hydrated cement and N-A-S-H

gels in alkali-activated aluminosilicate systems (Section 6).

A special chapter is dedicated to interfacial zones since nanoindentation is the only technique that can mechanically sense differences between fine inclusions like grains, aggregate, fibers and the composite matrix (Section 7). Extension to plastic and visco-elastic properties is covered in Section 8 where results of spherical indentation and dynamic indentation modes are used to disclose otherwise inaccessible properties of non-cementitious but similarly heterogeneous cell walls of a metallic foam or biological materials of bone cells and eggs.

Latest developments in nanoindentation of structural materials was made with relation to special sample preparation techniques like focused ion beam milling (FIB). Microscale sample prepared with FIB made possible to access intrinsic strength and fracture properties at scales as low as one micrometer. Information gained at this scale provided useful input data for multiscale models and for both up-scaling and down-scaling of mechanical properties to other composite levels. The achievements gained with nanoindentation in this field is summarized in Section 9.

3 Principles of nanoindentation

Nanoindentation is a micromechanical experimental technique that is capable of material characterization at very small volumes, typically nm^3 to μm^3 . Its basic principle lies in bringing a very small (usually diamond tip) to the sample surface, making an imprint and simultaneous registering force and displacement curve [12, 13]. Typical loading curves obtained from indentation on cement paste are shown in Fig. 1. The technique allows to perform surface impression tests at the scale that is appropriate for extraction of e.g. elastic modulus, hardness or short-term creep of lower level cementitious composite constituents (e.g. [14, 15, 16, 4]) but cannot give directly values of tensile strength and fracture energy that need to be tested in modes where significant tension stresses are developed (e.g. direct tension or bending). But nanoindenter can be used also as a loading tool of small scale (micrometer) specimens and can measure their load-deflection response with high accuracy. The small scale specimens can be prepared with advanced sample preparation techniques based on FIB milling (e.g. [17, 18, 19]). The technique allows precise fabrication of micrometer sized specimens within a cement paste [10].

Different kinds of probes can be used for making an imprint into the material surface [12]. The most popular one is the Berkovich tip which is a three-sided pyramid whose shape is close to rotational symmetrical bodies, Fig. 2. Theoretically, it produces constant

strain under the tip regardless the indentation depth and is used for assessing hardness and elastoplastic properties and in special cases also for fracture. Sharper indenters (cube corner) are more suitable for fracture initiation. Smaller but variable strains are induced by spherical tips. The main advantage of nanoindentation compared to classical mechanical tests is that a very small material volume having typically the order of several tens of nanometers can be accessed with the tip of the nanoindenter and material properties can be evaluated for such a small piece of the material.

Since the beginning of this century nanoindentation has emerged into matured tool that is standardly or even routinely used for characterization of various bulk or coating materials based on polymers, metals or biological samples (e.g. wood, bones). However, at early times, first generations of the machines were difficult to operate, calibrate and use in a proper manner. Thus, spreading of their utilization started just recently with great advancement in user friendliness, measurement speed and automatization of the acquisition procedures. Concurrently, in a similar time of nanoindentation genesis, multi-scale models started to be developed for various (cementitious) systems that are heterogeneous and hierarchical in their nature [20, 21, 22, 23]. Such models whose lowest level frequently coincide with the size of indentation were lacking of material characteristics and needed to be fed. Therefore, the connection of nanoindentation, heterogeneous systems of structural materials and multiscale models became to be natural and necessary.

As mentioned, tremendous development has been done in measurements as well as in modeling in the past twenty years. Identification of elastic and some inelastic properties of cement constituents, alternative binders, interfacial zones, metallic microstructures, wood and bone cells have been achieved. Due to enormous complexity given by material time-dependency and chemical (non)-integrity, variable stoichiometry and other problems some information is still missing and there is still a lot of room for progress in both measurements and modeling. This dissertation will guide the reader through partial

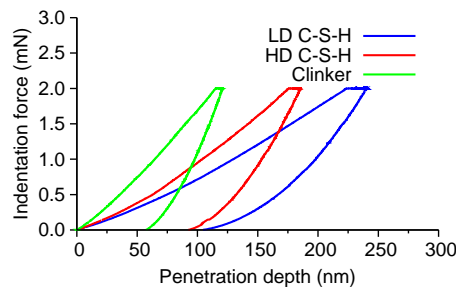


Figure 1: Typical load-displacement nanoindentation curves on cement paste.

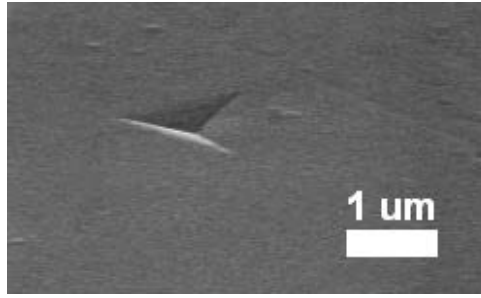


Figure 2: Imprint of Berkovich tip in hydrated cement paste.

achievements done in the specific field of nanoindentation of structural materials with emphasis on novelty that was accomplished at the time of publication.

4 Highlights of cementitious materials, alternative binders and their microstructure

Concrete is the most spread construction material in the world. Most of the concrete is composed of aggregate and cement which is an aluminosilicate binder that hydrates to form cement paste. Cement paste creates a matrix phase of various cementitious composites like mortars and concretes. Majority of the composites is prepared from Portland clinker whose hydration reaction and microstructure has been studied for a long time [24]. It has been widely acknowledged that cement paste has a hierarchical microstructure with variable chemistry and morphology across various scales. Cement is available in the form of finely ground powder (clinker) rich of Ca, Si, Al, O and other elements. In cement chemistry, C stands for CaO , S for SiO_2 , A for Al_2O_3 , F for Fe_2O_3 and H for water. Four basic clinker minerals can be found in Portland cement, namely C_3S , C_2S , C_3A and C_4AF .

Cement reacts with water and forms Calcium-silicate-hydrates (C-S-H) and calcium hydroxide (CH) as the main hydration products while substantial heat is released. The stoichiometry of C-S-H in cement paste is variable as well as the amount of chemically and physically bound water in its structure. Microstructural changes occur in C-S-H globules due to drying causing partially reversible shrinkage. The volumetric changes have been extensively studied by Jennings [25, 26] based on sorption-desorption isotherms. Jennings showed that the water leaves interlayer spaces upon drying. A strong hysteresis was observed at pressures below 11% r.h. The removal of water from the interlayer space causes the globules to collapse and increases their density. The density for d-dried C-S-H

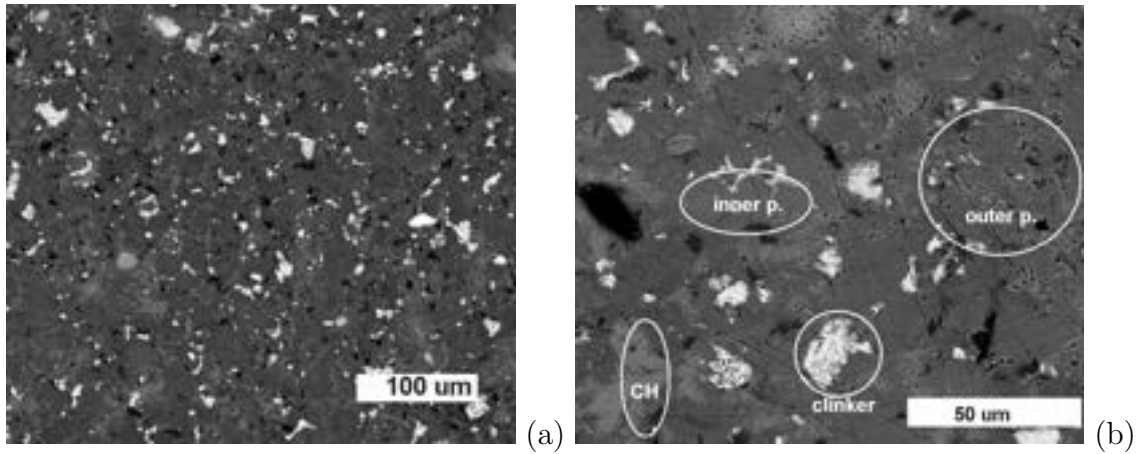


Figure 3: (a) SEM-BSE micrograph of cement paste. (b) Higher magnification image showing individual phases.

was measured to be 2850 kg/m^3 [27] which corresponds to $\text{C}_{1.7}\text{SH}_{1.3-1.5}$. At about 11% r.h. the globule composition is $\text{C}_{1.7}\text{SH}_{\sim 2.0}$ with the density of about 2450 kg/m^3 [28]. Saturated globule $\text{C}_{1.7}\text{SH}_{4.3-7.6}$ has the density of $1730-1960 \text{ kg/m}^3$ [29]. The water can further leave gel space upon heating causing further shrinkage and densifications.

From the morphological and also mechanical point of view, the pure chemical phases are often mixed on scales that are accessed by usual experimental techniques like SEM and also nanoindentation. Thus, a different nomenclature for hydration products have been coined in the past. Widely accepted terminology now include outer and inner products [30]. These products can be distinguished in SEM images. The inner product (mainly high density C-S-H (C-S-H_{HD}) mixed with other hydrates) occurs as rims around anhydrous clinker particles or is located at the places of former clinkergrains past full hydration. The phase is characterized by dark gray color in the back-scattered electron (BSE) mode of SEM micrographs. The outer product (mainly low density C-S-H (C-S-H_{LD}) regions mixed with other hydrates) are places of lighter gray color with visible submicron porosity. The outer product is often mixed with other phases like large CH crystals and clinker remnants that are the brightest areas seen in BSE images. Inner product forms less portion of the sample volume ($\sim 28\%$) while more porous outer product forms majority of the sample volume ($\sim 50\%$). Large Portlandite crystals (CH) appear in the microstructure ($\sim 10\%$). The rest of the volume is occupied by unhydrated clinkers ($\sim 3\%$) and capillary porosity ($\sim 12\%$), see [10] for details. The situation is illustrated in Fig. 4. Another example of typical cement paste SEM-BSE micrographs is shown in Fig. 3.

From the modeling point of view, the hierarchy of the cementitious matrix is usually

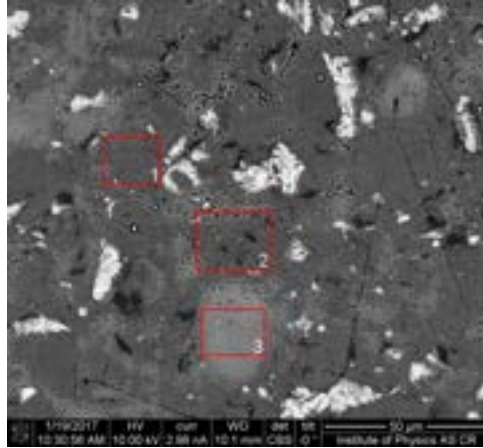


Figure 4: Microstructure of cement paste (1=inner product with C-S-H_{HD}, 2=outer product with C-S-H_{LD}, 3=CH).

treated with three microstructural levels.

1. **The C-S-H level.** The level consists of calcium-silicate globules that are, in fact, clusters with internal sheet like structure [31, 25, 26] and gel space (porosity < 10 nm). Globules are nearly spherical units of about 5 nm in diameter. The globules pack together in two characteristic packing densities, high (C-S-H_{HD}) and low (C-S-H_{LD}) [26]. The average packing density of the HD structure is 0.74 while it is less than 0.64 for the LD structure [25, 32, 26]. Such findings were demonstrated also by nanoindentation [33]. The characteristic size of the level spans the range of 1-100 nm.
2. **Cement paste level.** The level contains C-S-H gels, other hydration products like CH, C-A-H, ettringite-AFt, monosulfate-AFm, unhydrated clinker and capillary porosity [24, 28, 30]. The characteristic size of the level spans the range of 100 nm - 10 μ m.
3. **Cement paste with defects and air.** At this level, cement paste is enriched with defects in the form of cracks and entrained or entrapped air voids. The characteristic size range for this level is 1 μ m - 1 mm.

Next composite levels include aggregates, pores, defects and interfacial zones between the phases [22].

The C-S-H phase is responsible for major cement paste engineering properties like elasticity, strength but also time-dependent properties like aging and creep. The globules

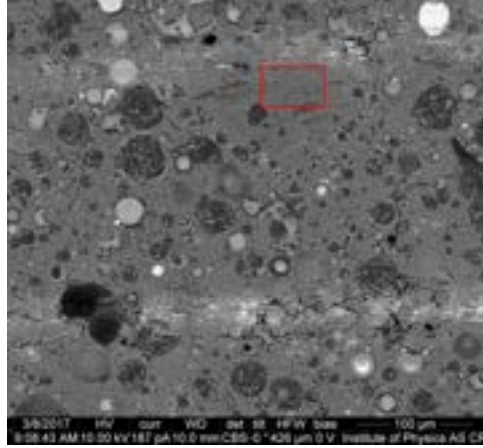


Figure 5: Microstructure of AAFA (rectangle shows a N-A-S-H gel region).

consist of solid C-S-H and internal water. Microstructural changes occur in globules due to drying causing partially reversible shrinkage. From the morphological and also mechanical point of view, the pure chemical phases are often mixed on scales that are accessed by usual experimental techniques like SEM and also nanoindentation.

One of the alternative binders used in concrete industry is the fly ash. Fly ash is produced as a by-product in brown coal power plants. It can be used as a filler that partially reacts in alkaline concrete environment and reduces the amount of cement. Or, fly-ash can be used as a precursor for preparation of alkali-activated materials (AAFA) that are characterized with similar reaction product to C-S-H gels, the sodiumaluminosilicate gel (N-A-S-H gel). Microstructure of AAFA samples is more complex in comparison with cement. It consists of the main reaction product, the N-A-S-H gel, non-reacted and partly reacted slag grains, non-reacted glass particles and multi-level porosity [2]. Typical microstructure with the N-A-S-H region is shown in Fig. 5.

5 Elastic properties and creep effects in cementitious materials

There has been a few popular methods for evaluation of bulk elastic properties of a homogeneous materials from nanoindentation. Probably the most popular and widely used is the one authored by Oliver and Pharr [34]. The theory derives reduced modulus

from analytical solution of isotropic elastic half-space punched by a rotational body as

$$E_r = \frac{1}{2\beta} \frac{\sqrt{\pi}}{\sqrt{A_c}} \frac{dP}{dh} \Big|_{h=h_{max}}, \quad (1)$$

where $\frac{dP}{dh}$ is the contact stiffness assessed as the slope of the indentation unloading branch (Fig. 1) at the maximum depth h_{max} , A_c is the projected contact area of the tip at peak load, and β is the geometrical correction factor introduced to correct the non-symmetrical indenter shape ($\beta=1.034$ for the Berkovich tip). The effect of non-rigid indenter is taken into consideration by the following equality

$$\frac{1}{E_r} = \frac{1 - \nu^2}{E} + \frac{1 - \nu_i^2}{E_i}, \quad (2)$$

where E and ν correspond to the elastic modulus and Poisson's ratio of the tested material, respectively. E_i and ν_i are the parameters of the indenter ($E_i=1141$ GPa and $\nu_i=0.07$ for diamond). Another material quantity, the hardness H , representing the mean contact pressure under the indenter can readily be obtained from load-penetration indentation curves as

$$H = \frac{P}{A_c}. \quad (3)$$

The reason for a great popularity of the method lies in the fact that the method removes complicated calibration of the tip shape. The method was tested mainly on metals by the authors with satisfactory results. But soon after publication of this methodology, many problems connected with its assumptions have been identified. E.g. effects of sinking-in or pilling-up were identified on materials that do not comply with the theoretical assumptions. Due to large strains that are developed under the indenter and due to the development of geometrically necessary dislocations under the tip standard evaluations led to so called indentation size effect [35]. On the other hand, other sources of size effect like surface roughness, hardening caused by surface preparation and other reasons have been identified as well.

For the case of cementitious materials the elastic solution relies on the fact that the material is time-independent and does not creep. This is not the case of all cementitious and other structural materials that exhibit large creep deformation especially under high strains. This effect of creep on evaluation of intrinsic elastic properties on cement was firstly recognized in [1], where an artificial source of size effect on hydrated cement paste was diagnosed, Fig. 6. Multi-cycle indentation and variable dwelling periods have been used to study this effect. Since the creep has been found to be logarithmic since the beginning of the load, using longer dwelling times led to creeping out of the material and

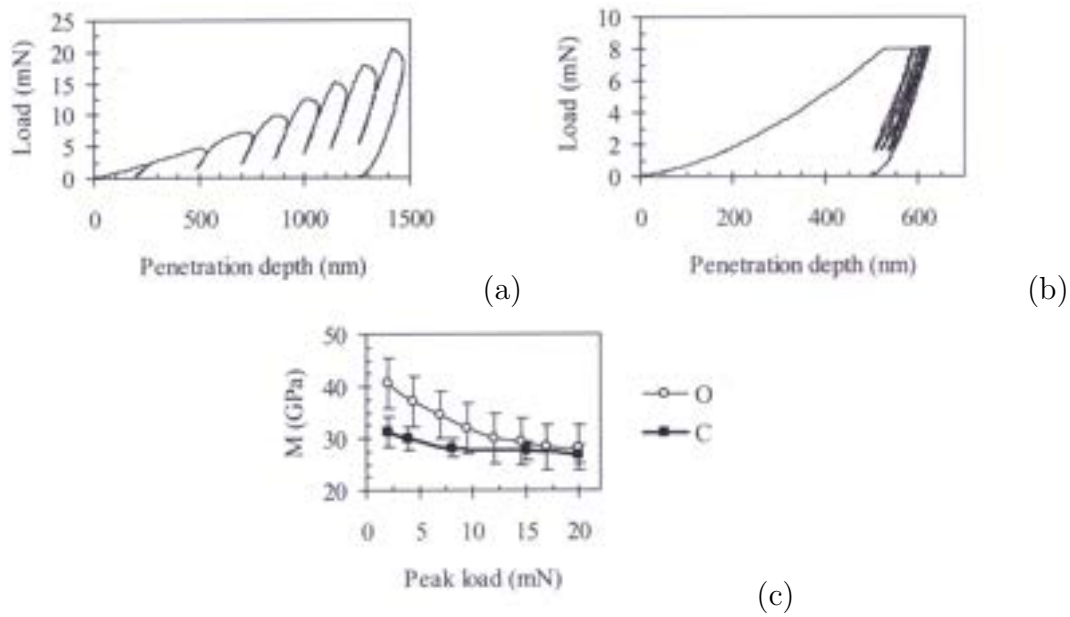


Figure 6: Examples of loading diagrams for (a) series “O”—multiple loading cycles with increasing load 2–20mN with no dwell period at peaks; (b) series “C”—5 loading/unloading cycles to the same load (8 mN) with a dwell period at the peak of 120 s; (c) indentation moduli for the series. After [1].

diminishing of this size effect. Similar behavior was encountered on polymeric sample giving us the proof of common visco-elastic character of both hydrated cement and polymer materials. The remedy for removing of the artificial size effect on cement given by the paper [1] was to increase dwelling time used in standard load-unload experiments. This simple finding helped other researchers to properly identify elastic properties on little or moderately creeping materials such as on cement pastes. Without controlling this parameter many studies done on various scales were burden by an error.

At the early times of investigations on hydrated cement pastes no or simple distinction was made between individual low-scale constituents. Some of the early studies identified clinker elastic properties [36] made ex-situ, e.g. on unhydrous clinker minerals out of cement paste. In hydrated paste, part of the clinkers is consumed by hydration reaction. Thus, mechanical properties of the paste must be distinguished for hydrated phases, unhydrated rest of clinkers and, if any, transitional zones between the constituents. It was proved by Němeček [1] that creep properties can only be attributed to fully unhydrous clinkers while all creep takes place in hydrated part, Fig. 7.

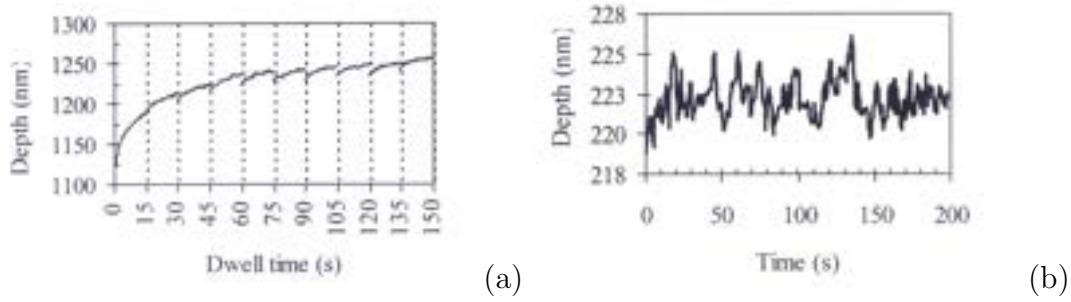


Figure 7: Example of creep deformation in (a) hydrated cement and (b) steady deformation of a clinker. After [1].

6 Nanoindentation on heterogeneous microstructures

Traditionally, mechanical properties of materials are assessed from macroscopic tests on samples with centimeter to meter dimensions. Such measurements can only describe overall (averaged) properties of the whole like overall Young's modulus or overall strength. Continuous attempts to characterize material microstructure and mechanical properties of smaller volumes led to the development of micro- and nanoindentation. Measurements on substantially smaller materials volumes firstly used an assumption of homogeneity in the indentation volume and in its surroundings. Nanoindentation was used for characterization of macroscopically homogeneous materials such as glass, metals, ceramics etc. With the development of indentation, analytical solutions with simplified assumptions have been derived. As mentioned, Oliver and Pharr [34] procedure assuming indentation of rotational bodies in an elastic half-space with flat surface is mostly used evaluation procedure to date.

However, structural composites such as concrete, cement paste, gypsum, metals and others are characterized by a heterogeneous microstructure at different length scales (nm to m). Thus the heterogeneity becomes important also at the scale of indentation. As a direct solution of the problem indentation can be performed on individual phases whose volume is larger than the indentation volume. This is, however, possible only in limited number of cases. For example, hydrated phases in cement paste are mostly amorphous (C-S-H gels) with variable density, variable stoichiometry, but common chemical composition and homogeneous-like regions can not be fully detected e.g. by electron microscopy (BSE, EDS) or by optical microscopes that are attached to nanoindentors. Thus, it is uneasy to perform dedicated indentation to a single phase and novel methods had to be developed.

Very useful idea of **statistical grid indentation** was firstly used by Constantinides and Ulm on cementitious systems under calcium leaching conditions [33]. Statistical

deconvolution based on evaluation of data from large indentation grids was applied [15]. The statistical grid indentation was used by Němeček et al. [4] for identification of various heterogeneous structural materials including *cement paste, gypsum and aluminium alloy* and good applicability was proved. A mathematically *ill-posed problem of deconvolution* into infinite number of phases was solved by a priori determination of finite phase number by combining information gained from sample chemistry and SEM. A choice of specific length scale for indentation was derived from porosity measurements since porosity was identified as a key factor influencing scaling of material properties in individual phases. A specific deconvolution procedure with assured convergence was developed in [2] with the following main steps. Experimental histograms are constructed from all measurements whose number is N^{exp} , using equally spaced N^{bins} bins of the size b . Each bin is assigned with a frequency of occurrence f_i^{exp} that can be normalized with respect to the overall number of measurements as f_i^{exp}/N^{exp} . From that, we can compute the experimental probability density function (PDF) as a set of discrete values:

$$P_i^{exp} = \frac{f_i^{exp}}{N^{exp}} \cdot \frac{1}{b} \quad i = 1 \dots N^{bins} \quad (4)$$

The task of deconvolution into M phases represents finding $r = 1 \dots M$ individual PDFs related to single material phases. If we assume normal (Gauss) distributions, the PDF for a single phase can be written as:

$$p_r(x) = \frac{1}{\sqrt{2\pi s_r^2}} \exp \frac{-(x - \mu_r)^2}{2s_r^2} \quad (5)$$

in which μ_r and s_r are the mean value and standard deviation of the r -th phase computed from n_r values as:

$$\mu_r = \frac{1}{n_r} \sum_{k=1}^{n_r} x_k \quad s_r^2 = \frac{1}{n_r - 1} \sum_{k=1}^{n_r} (x_k - \mu_r)^2 \quad (6)$$

and x is the approximated quantity, i.e. the E modulus in our case. The overall PDF covering all M phases is then:

$$C(x) = \sum_{r=1}^M f_r p_r(x) \quad (7)$$

where f_r is the volume fraction of a single phase:

$$f_r = \frac{n_r}{N^{exp}} \quad (8)$$

Individual distributions can be found by minimizing the following error function:

$$\min \sum_{i=1}^{N^{bins}} [(P_i^{exp} - C(x_i)) P_i^{exp}]^2 \quad (9)$$

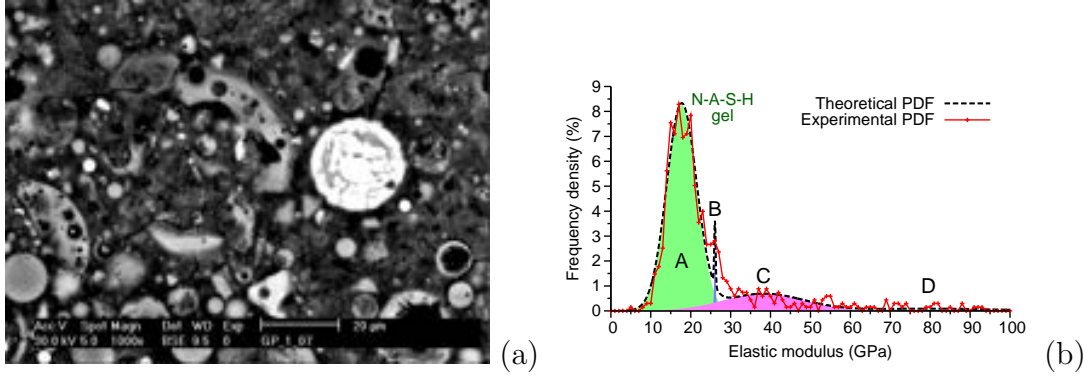


Figure 8: (a) AAFA microstructure and (b) histogram of elastic moduli with deconvolution to individual phases. After [2].

in which one computes quadratic deviations between experimental and theoretical PDFs in a set of discrete points that is further weighted by the experimental probability in order to put emphasis on the measurements with a higher occurrence.

The work conducted in [2] revealed, for the first time, intrinsic mechanical properties of **N-A-S-H gels** that form binder phase of alkali-activated aluminosilicate materials, sometimes called geopolymers (Fig. 8). The procedures were applied to activated fly-ash and pure activated metakaoline in two thermally treated variants. The deconvolution led to the same phase properties but different reaction kinetics in thermal treatment caused different volumetric ratios between the phases.

Later, the procedure was successfully applied to microstructures with stochastic distribution of amorphous or crystalline phases such as the cement paste, gypsum and aluminium alloy [4]. In the later paper, not only phase properties and volume fractions derived from statistical deconvolution were presented but also micromechanical homogenization of a representative volume was used stiffness matrix. Simple analytical homogenizations like Mori-Tanaka or self-consistent schemes [37] were used and compared to general FFT-based homogenization [38]. The FFT-based homogenization uses regular discretization grid and material parameters are only needed in the grid points. Such discretization matches with grid nanoindentation that provides material characteristics at the points. Fast Fourier transformation (FFT) is applied to integral Lippmann-Schwinger equation which decomposes strains into homogeneous (average on domain) and polarization (fluctuating) parts as:

$$\epsilon(\mathbf{x}) = \frac{1}{\Omega} \int_{\Omega} \epsilon(\mathbf{x}) d\mathbf{x} - \int_{\Omega} \Gamma^0(\mathbf{x} - \mathbf{y}) : (L(\mathbf{y}) - L^0) : \epsilon(\mathbf{y}) d\mathbf{y} \quad (10)$$

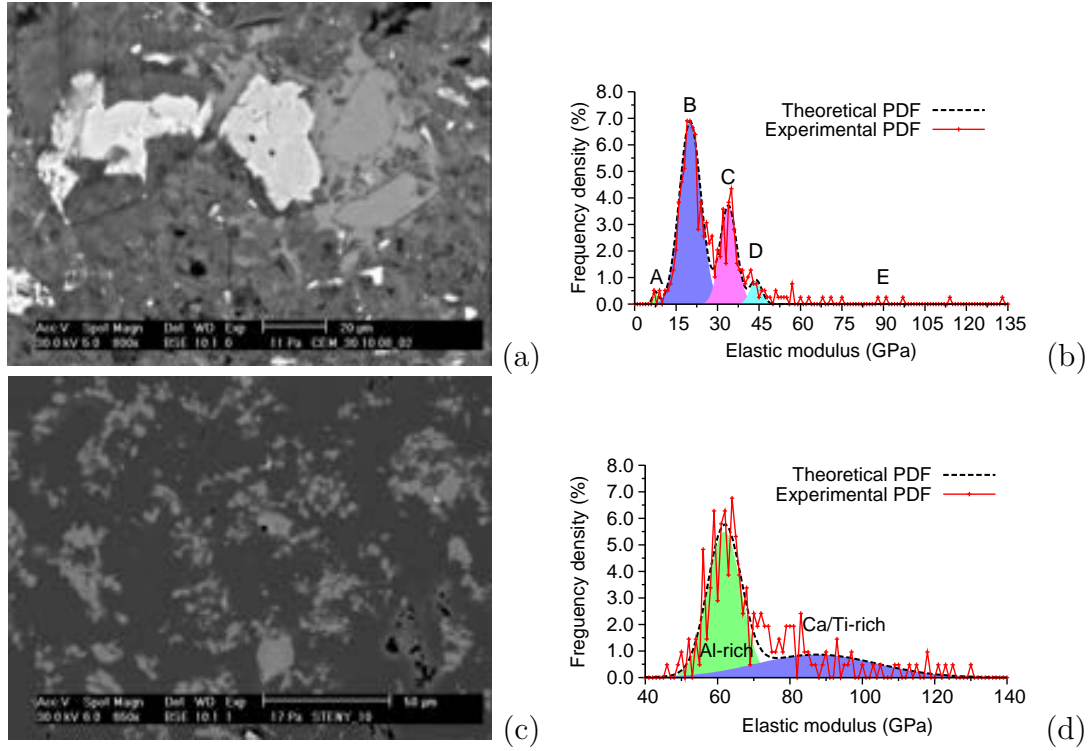


Figure 9: (a) Hydrated cement microstructure, (b) histogram of elastic moduli with deconvolution to individual phases, (c) microstructure of a cell wall of Al foam and (d) deconvolution on Al-foam. After [4].

in which ϵ and L stand for the local strain and stiffness tensor, respectively, Γ^0 is the periodic Green operator associated with the reference elasticity tensor L^0 being a parameter of the method [38, 39]. The solution of the problem is found after discretization by trigonometric collocation method [39] which leads to the non-symmetrical linear system of equations [40, 41] in which material coefficients at discretization points (elastic moduli) and macroscopic strain are used as inputs. Finally, effective stiffness matrix is calculated from averaged stresses and strains in the domain [41, 4]. In the paper of Němeček et al. [4], the FFT-homogenization was firstly used to derive homogenized elastic stiffness matrices for given heterogeneous systems.

Later, the application of deconvolution and homogenization was successfully used for solving problems on several length scales of materials with even more complex microstructures, e.g. high-strength cementitious composites [5]. High performance material consists of multiple raw phases like cement, fly-ash, aggregates, water and admixtures. Heterogeneity is given by these components themselves as well as hydration reactions that form matrix for this composite. The methodology of statistical grid indentation and prediction

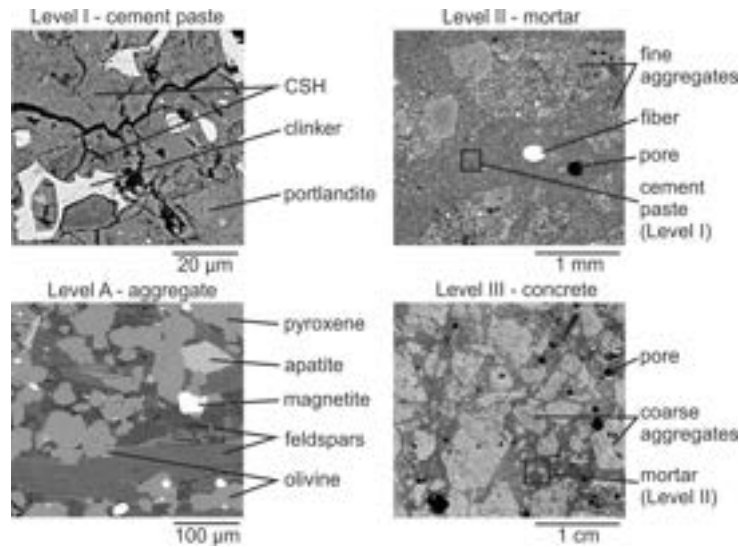


Figure 10: Separation of levels in the multi-scale model of UHPC. After [42].

of elastic stiffness via analytical methods and FFT-homogenization at several scales have been proved over standard dynamic tests. Similarly, micromechanical homogenization on ultra-high performance concrete (UHPC) was done including analysis of multi-phase basalt aggregate composing of phases like pyroxene, apatite, olivine, feldspar and magnetite (Fig. 10). Cement paste as a binder was again homogenized from individual phases at two levels [42].

7 Interfacial transitional zones

Individual phases in structural composites are often accompanied with transitional zones in which variable density, stoichiometry or porosity appears in comparison to bulk. The so called, interfacial transitional zones (ITZs) can be detected around mineral aggregates, residual clinker minerals, around any inclusions (e.g. reinforcement, fibers, etc.). Although, ITZ usually occupies only a fraction of the total composite volume, its mechanical behavior is crucial for overall elastic and mainly inelastic properties of the whole. Many researchers studied chemical and physical properties of ITZs of cementitious systems (e.g. [30]) but the most precise measurement can be performed with nanoindentation. Novel or historic materials bring challenges in the form of variable ITZ and nanoindentation is, therefore, the best investigator's choice when studying mechanical response of individual phases and composite responses. Lime-based mortars containing crushed clay bricks used in history is a perfect example of such material with the importance of ITZ [8]. The

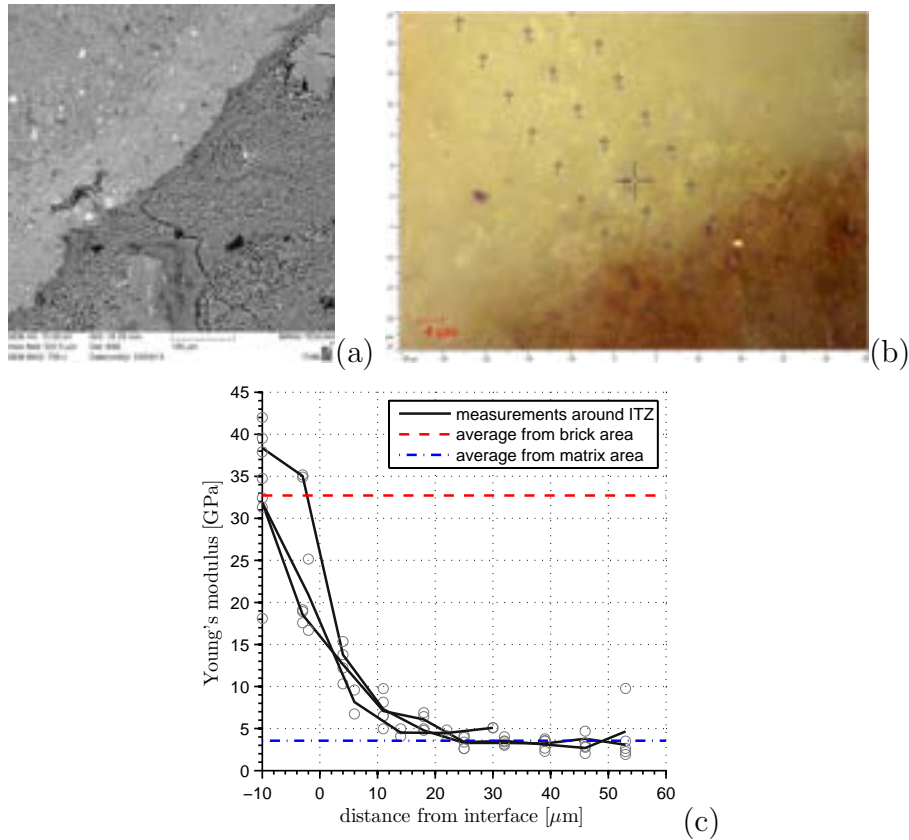


Figure 11: (a) SEM micrograph of brick rim, (b) light optical image with prescribed indents, (c) evolution of Young's modulus in ITZ. After [8].

interface between the lime-based matrix and brick fragments was investigated (Fig. 11). Evolution of elastic modulus in ITZ combined with SEM-EDS analysis gave unique values used later as input values of a hierarchical multi-scale model of composite strength [43]. Other type of ITZ was investigated in [44] on fiber-reinforced concrete. The evolution of mechanical properties in ITZ is well documented for elastic properties as well as viscous properties showing creep compliance functions different from the bulk [45].

8 Plasticity, visco-elastic properties and dynamic nanoindentation

After in-depth investigations of elastic properties of individual phases of cementitious and other composites the nanoindentation technique has matured and other types of inelastic properties could be researched together with the advancement in nanoindenter instrumentation. Local mechanical characterization may employ spherical indentation that leads to

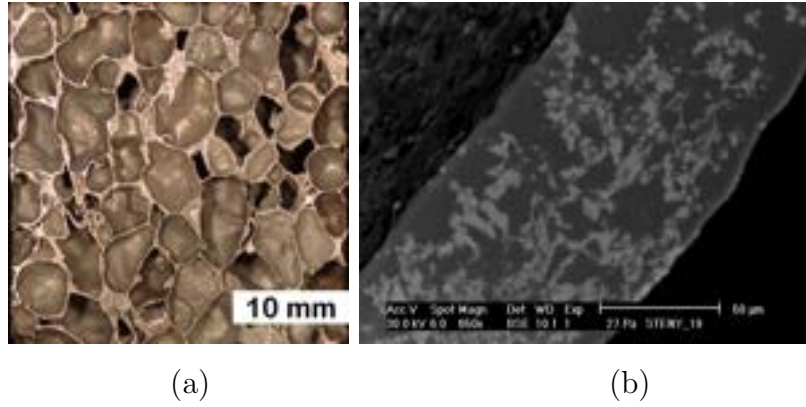


Figure 12: Microstructure of Al foam. (a) Optical image showing large pores. (b) SEM image showing heterogeneous cell wall. After [7].

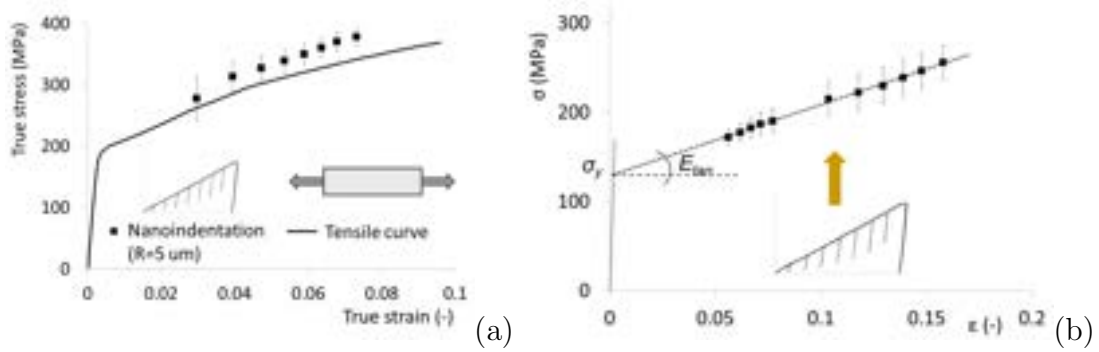


Figure 13: Stress-strain relations obtained by nanoindentation compared with tensile test on (a) aluminum alloy EN AW 6060 and (b) Alporas cell wall. After [46].

assessment of plastic properties such as yield strength. Such characteristics, typical for metals, were investigated by nanoindentation on a material that is hard to describe on macroscopic scale, the metal foam. Metal foam is a hierarchical porous material with very thin solid walls, typically a hundred micrometers (Fig. 12). Identification of stress-strain relation of aluminium foam cell wall was provided by nanoindentation and published in [6, 46] (Fig. 13). Approaches of statistical indentation, analytical and numerical homogenization on different scales of the foam were combined and employed in [7]. FE model for the upper foam level is shown in Fig. 14.

Not only static nanoindentation but also dynamic indentation [47] is capable of giving valuable information on material inelastic, namely visco-elastic properties. The dynamic indentation (nanoDMA) is described by a simple one-degree-of-freedom oscillator which includes the sample stiffness K_s and the damping C_s , as well as the stiffness K_i and

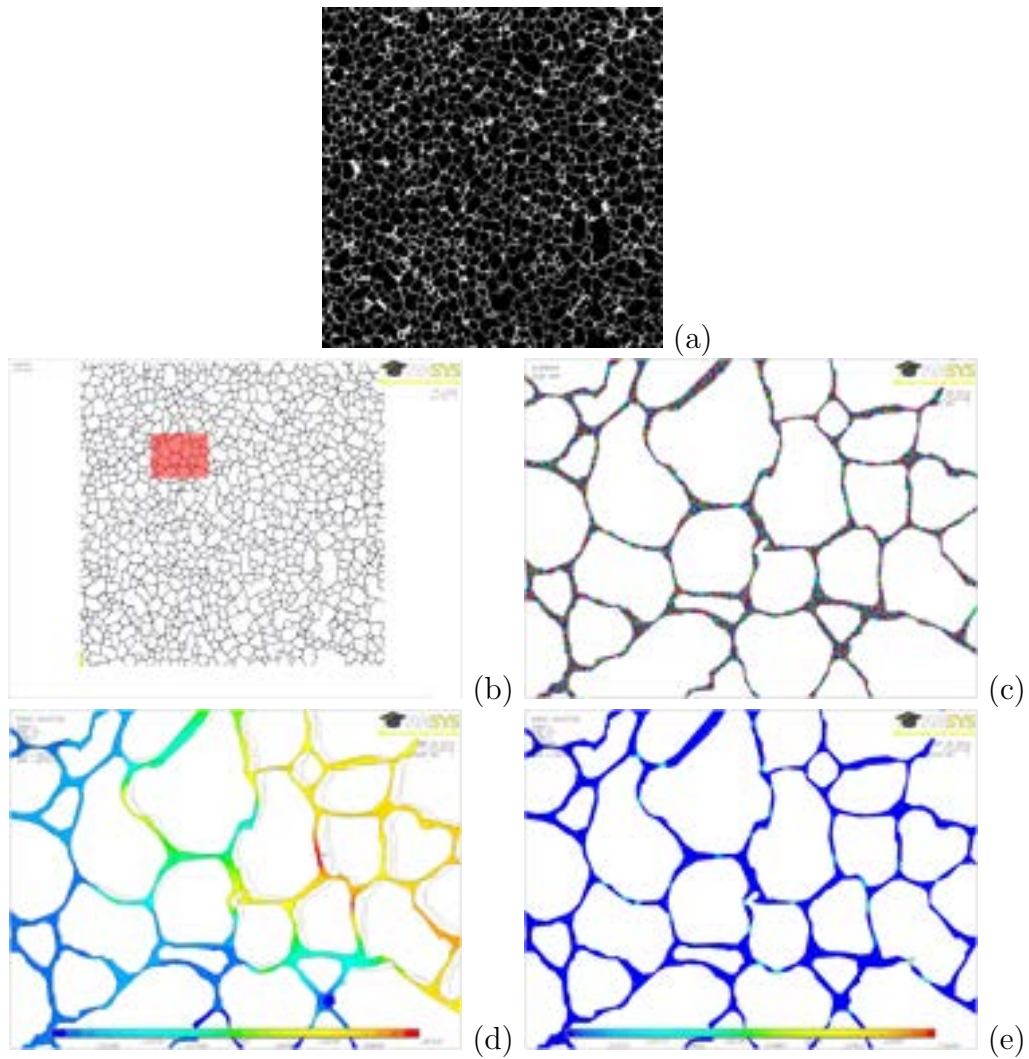


Figure 14: (a) Original high resolution foam scan (domain size $106.4 \times 106.4\text{mm}$). (b) FE mesh on the whole domain. (c) Detail of FE mesh from (red rectangle in figure (b)). (d) Detail of axial deformations and deformed shape in uniaxial compression (loaded in horizontal direction). Plotted at overall axial strain= 0.004717. (e) Detail of equivalent plastic strains. After [7].

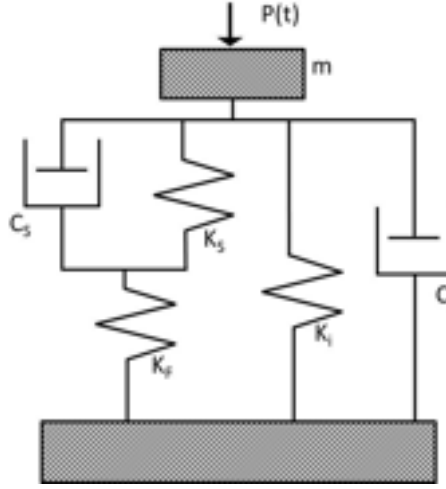


Figure 15: Dynamic model of the indenter system in contact with specimen where m is the indenter mass, C_i is the damping coefficient of the indentation system in ambient air, C_s is the damping coefficient of the specimen, K_s is the contact stiffness, K_i is the spring constant of the leaf springs that hold the indenter and K_F is the frame stiffness ($K_F \rightarrow \infty$).

the damping C_i of the indentation system, see Fig. 15. Two visco-elastic properties, the storage (E_r) and loss (E_l) moduli [47] are derived as

$$E_r = \frac{K_s \sqrt{\pi}}{2\sqrt{A}} \quad E_l = \frac{\omega C_s \sqrt{\pi}}{2\sqrt{A}}. \quad (11)$$

On metal foam, dynamic indentation was successfully applied [6] to distinguish between microstructural phases originating from production process of the foam that includes incorporation of CaO and TiO₂ as viscosity and foaming agents and the aluminium matrix (Fig. 16).

Plasticity and visco-elasticity is also characteristic for polymers. Such response appears also on microscale as documented in [3]. Information obtainable from nanoindentation tests such as apparent modulus, hardness and components of creep compliance function are described in [3]. It was found that the arrangement of tests (indenter shape, creep compliance function and test duration) must be chosen with respect to the purpose of measurement. High stresses under a pointed indenter cause irreversible plastic and viscous deformations. If only low stresses are expected in applications, spherical indenters and low loads are better.

Similarly to metal foam whose cell walls are hardly accessible by any other mechanical tool but nanoindenter trabecular bone tissues can be explored by nanoindentation.

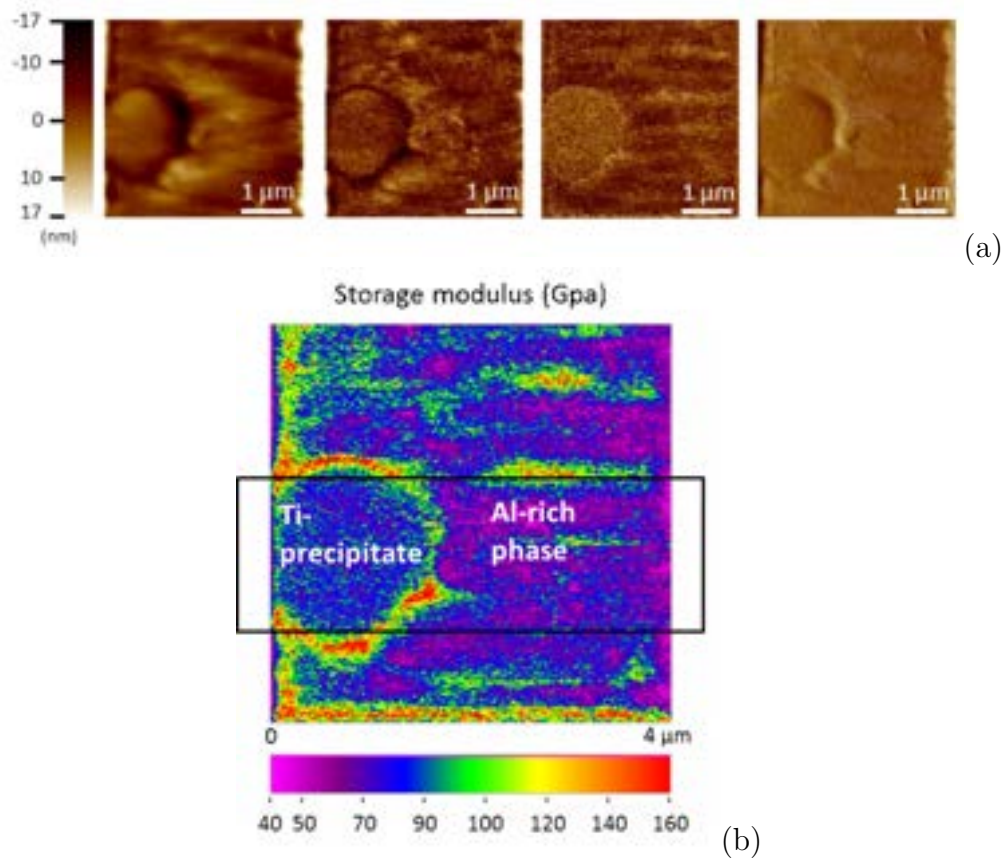


Figure 16: (a) Scan image obtained by in-situ imaging (left to right: topography; amplitude of the tip displacement; phase shift of the displacement with respect to the driving force; gradient of the tip displacement). (b) Storage modulus map (in GPa). After [6].

The trabecular cells were measured by static and dynamic indentation to get average visco-elastic properties of the tissue and further used in e.g. finite element models [48]. Nanoindentation is attractive also for characterization of more exotic biological materials such as eggs. Local differences and anisotropic stiffness characteristics of hen's eggshells were identified in [49].

Back to the cementitious systems, visco-elastic behavior can be encountered for hydrated C-S-H phases instantly after imposing the load. Thanks to the nanoindenter, the time-displacement curve can be monitored and viscous properties evaluated. Standardly, the creep indentation parameter (*CIT*) is used for comparison of different creep responses. The *CIT* is evaluated from holding periods of trapezoidal loading functions used in standard indentation and is defined as

$$CIT(P, t_1, t_2) = \frac{h(t_2) - h(t_1)}{h(t_1)} \times 100 \quad (12)$$

and reflects a relative change in indentation depth, h , gained in holding period of (t_1, t_2) seconds. The CIT is dependent on the contact force P duration of the holding period. But, it is a simple and useful property that can be used for comparison between the phases or samples. On cement paste, different CIT can originate e.g. from locations in ITZ and bulk ([45]). Yet simple analytical expression can be used to fit creep compliance function $J(t)$ as

$$J(t) = \frac{2h^2(t)}{\pi(1 - \nu_s^2)P_0 \tan \alpha} \quad (13)$$

where $h(t)$ is depth of indent in time t , P_0 is load, ν_s Poissons ratio of sample and α is the angle between surface and edge of the tip (for Berkovich tip $\alpha = 19.7^\circ$). The simple formula of Eq. 13 assumes step loading function which is in practice replaced by fast loading, long holding and fast unloading periods. An example of various creep compliance functions evaluated in ITZ around steel fiber in cement matrix is shown in Fig. 17.

9 Strength properties

Perhaps, the most challenging characteristics of materials that are simultaneously one the most important engineering properties are material strength and fracture toughness. For a long time, strength characterization was restricted to samples with large dimensions. Problems connected with scaling of strength and fracture energies of concrete were in-depth studied by Bažant and co-workers [50]. Naturally, the strength of smaller material

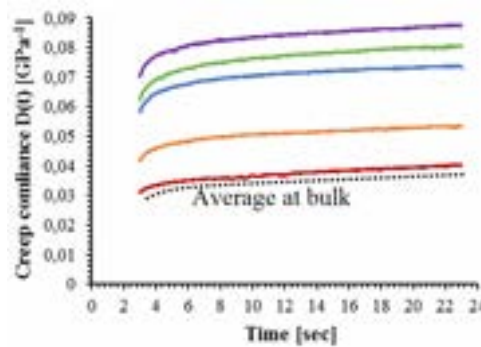


Figure 17: Creep complinace functions of the bulk (dotted black line) and around steel fiber (color curves). After [45].

volumes or microstructural constituents varies significantly from its macroscopic counterparts. Employing nanoindentation for strength or fracture is, however, not possible in a standard manner in which an indenter is press into the sample surface. Such conditions impose high strains and cause fracture deformation which is hard to identify.

Attempts have been performed by the author to assess fracture toughness from indentation fracture around indents combining information gained from an indenter and from FIB sectioning (i.e. physical tomography) made on the sample of hydrated cement [9]. From FIB-sectioning three-dimensional image of cracks could be identified, Fig. 18. Related fracture energy was deconvoluted from total indentation energy using simplified assumptions dividing the total energy into elastic, plastic, fracture and creep parts [9]. However, due to difficulties with sample sectioning and time demands the approach gave only the first estimates with limited reproducibility.

On the other hand, new approach based on direct measurement of microbeams loaded in bending with the aid of nanoindenter gave perfect results of both tensile strength and fracture energy related to individual constituents of cement paste. For the first time, Němeček et al. [10] assessed these characteristics for micrometer sized specimens fabricated by FIB in different types of C-S-H gels and calcium hydroxide. The FIB is a well established technique that uses a finely focused beam of gallium ions for precise micro-machining of various materials [17]. FIB milling procedure was optimized to suppress the redeposition of sputtered material on the micro-beam surface [18]. The final milling step was done at an accelerating voltage of 30 kV and a current of 1 nA. Examples of microbeams as fabricated by FIB are shown in Figs. 19, 20 and 21. Microbeams are firstly tested in an elastic regime and in the second stage, the micro-beam is progressively loaded by a constant displacement increment up to the failure. The tensile strength is

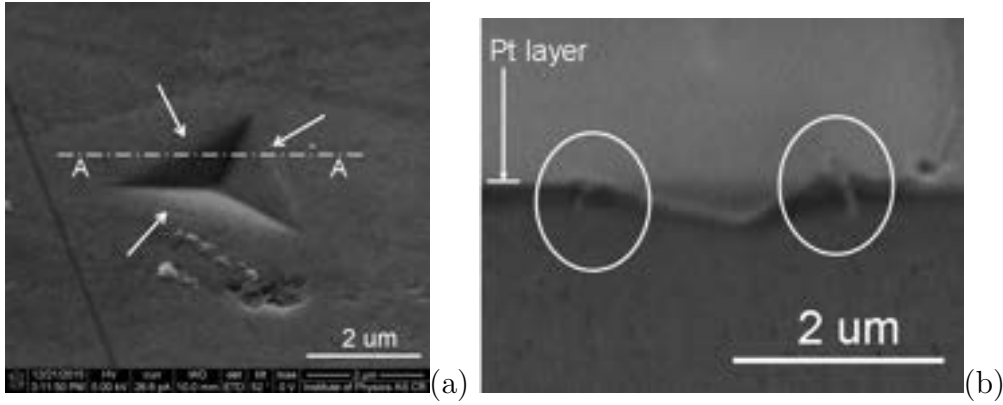


Figure 18: (a) An indent before sectioning. Cracks located around the indent are marked by arrows, (b) Cross section of an indent (indicated by dash-and-dotted line in a). Cracks are highlighted in circles. After [9].

calculated using the elastic theory of beams as

$$f_t = \frac{F_{max} L h}{I_y 3} \quad (14)$$

where F_{max} is the maximum force (measured by the nanoindenter), I_y is the second moment of inertia and h stands for the depth of triangular cross section (measured by SEM). Alternatively, three dimensional FE model can be used if the beam geometry is non-trivial. In [10], the susceptibility to the brittle failure of the beams was quantified by the supremum estimate of the total fracture energy computed as

$$G_f^{sup} = \frac{1}{A_f} \int_0^{w_{max}} F dw \quad (15)$$

where F is the force, w_{max} is the peak deflection and A_f is the fracture area. The supremum fracture energy is computed from the assumption that the micro-beam behavior shows neither snap-back nor softening and that the maximum force corresponds to the maximum energy release rate with a limiting stable crack propagation. The fracture area was approximated by the whole ligament area which, for a triangular cross section without a notch. Example of a fractured microbeam can be seen in Fig. 22. Later, the fracture energy was refined by performing experiments on notched beams [51]. In this case, three-dimensional FE model needed to be constructed to describe correctly geometry of the test and stress concentrations at the notch, Fig. 23.

Very consistent results with good reproducibility were obtained in [10]. Striking differences have been found for strength compared to macroscopic ones. The tensile strength

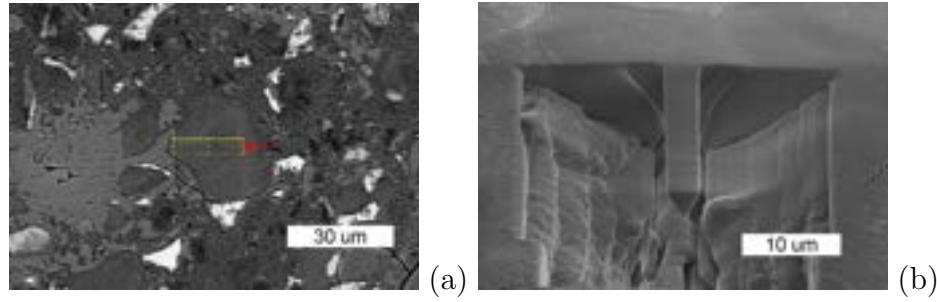


Figure 19: Cantilever micro-beam fabricated in the inner product. (a) Location before FIB milling labeled by the yellow rectangle. The red arrow indicates the fixed end position. (b) Front view of the cantilever after FIB milling. After [10].

assessed at the micrometer scale is in the order of hundreds of MPa which is two orders of magnitude higher with respect to usual lab scale (cm to m) characteristics, see Tab. 1.

Table 1: Elastic properties, hardness, tensile strengths and fracture energies of individual phases from micro-beam bending tests and from nanoindentation in the vicinity of micro-beams. After [10].

		Phase			Legend:
	Test type	Outer product	Inner product	CH	
E (GPa)	BB	23.9 ± 1.4	34.0 ± 1.9	39.2 ± 6.6	
	NI	24.9 ± 1.3	33.6 ± 2.0	39.0 ± 7.1	
H (GPa)	NI	0.98 ± 0.07	1.15 ± 0.11	1.37 ± 0.11	
f_t (MPa)	BB	264.1 ± 73.4	700.2 ± 198.5	655.1 ± 258.3	
G_f^{sup} (J/m ²)	BB	4.4 ± 1.9	19.7 ± 3.8	19.9 ± 14.4	

E =Young's modulus; H =hardness; f_t =tensile strength; G_f^{sup} =supremum of fracture energy;

NI=nanoindentation tests performed in the vicinity of the micro-beam; BB=beam bending

Unique data were published in [10] and two years after used in a multi-scale model of cement paste giving a prediction of composite tensile strength at a higher level [11]. The discrepancy between the scales was explained by fracture mechanics model incorporating microcracks of different origin in to the microstructure, Fig. 24. At the same time, fracture energies related to individual cement components were found to be in very good correlation to molecular dynamics simulations [52, 53].

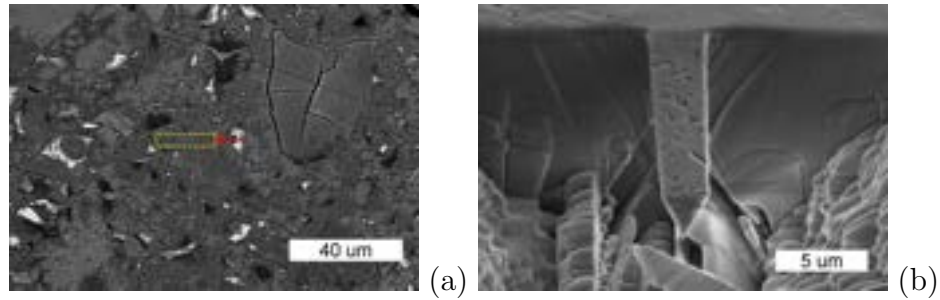


Figure 20: Cantilever micro-beam fabricated in the outer product. (a) Location before FIB milling labeled by the yellow rectangle. The red arrow indicates the fixed end position. (b) Front view of the cantilever after FIB milling. After [10].

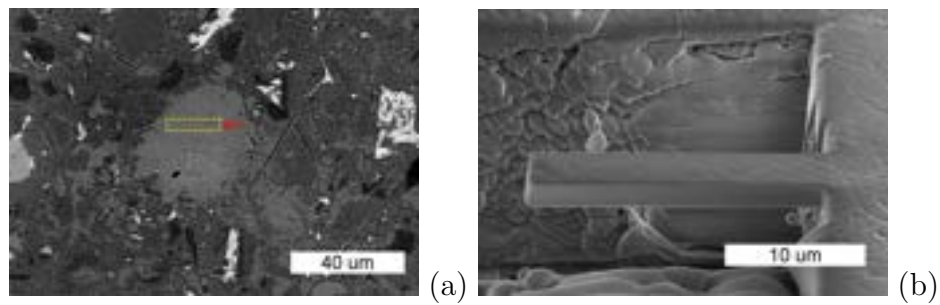


Figure 21: Cantilever micro-beam fabricated in CH. (a) Location before FIB milling labeled by the yellow rectangle. The red arrow indicates the fixed end position. (b) Side view of the cantilever after FIB milling. After [10].

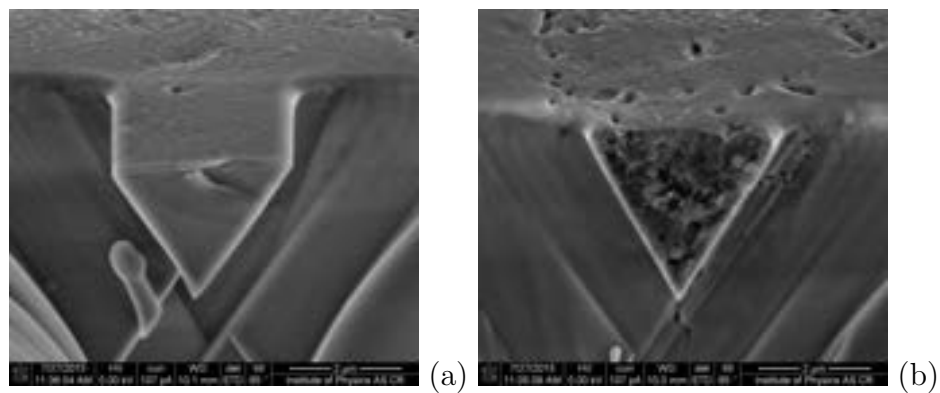


Figure 22: SEM micrograph of the fracture surface on (a) CH and (b) outer product micro-beams. After [10].

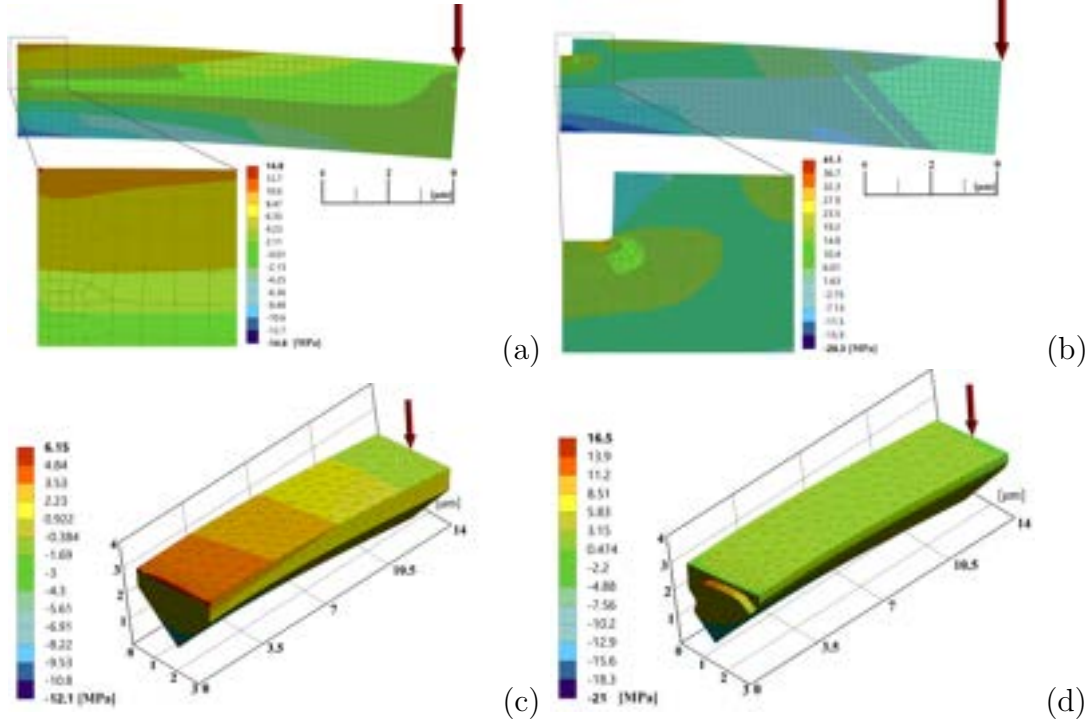


Figure 23: FE model of cantilever micro-beams. a) 2D un-notched, b) 2D notched, c) 3D un-notched, d) 3D notched. After [51].

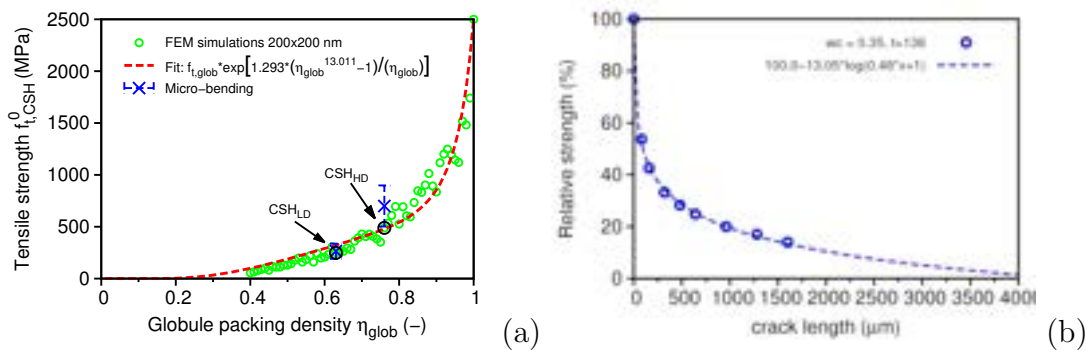


Figure 24: (a) Tensile strength scaling in C-S-H gel with various packing density of globules and (b) strength scaling in cement paste based on a crack size. After [11].

10 Conclusions and outlook

It has been demonstrated that nanoindentation is a powerful tool that brings new insights to the material and valuable inputs for methods of micromechanics and multi-scale models that need to be calibrated. Over the past twenty years, nanoindentation techniques has matured and measurements are now easier with more options. Elastic, visco-elastic and fracture properties can be assessed for very small material volumes. Complex microstructures of structural composites can be characterized mechanically and results of nanoindentation serve as a primary source of information for models that are spanning scales several orders of magnitude apart. Cementitious composites are a typical representatives of such systems that are, on the other hand, very important for building industry since cement and concrete are world number one construction materials.

Since pioneer times in 80's to 90's of the last century nanoindentation has changed dramatically. Very long manual calibration procedures, long measurement times and poor positioning systems from that times are now replaced with fast acquisition electronics and sophisticated systems compensating for thermal drifts automatically. In 2000, an approximate time for calibrating the indenter was in the range of hours to days. Performing a single static indent took around 10 minutes. Nowadays, the procedures are shorten to minutes or even seconds. Today's nanoindenters offer acquisition rates up to 30 kHz, in-situ scanning capabilities and high accuracy with drifts as low as 0.05 nm/s. That all speeds up new research. Nevertheless, some unique achievements in the field of cementitious composites were accomplished in the past by the author utilizing nanoindentation as an indispensable tool since the early times. This includes **creep effects** on evaluation of elastic properties [1], low-scale elastic properties of **N-A-S-H gels** in alkali-activated fly ash [2], development of unified methodology for assessing intrinsic elastic properties of individual phases and their **homogenization** applied to various composites [4, 5], identification of **ITZ properties** for specific composites [8, 44] and last, but not least, **strength and fracture properties** of individual cement constituents based on unique microbending experiments prepared by **FIB** [10]. The achievements were summarized in Section ?? and documented widely in this dissertation. It is assumed that the characteristics will be further used in new material models for new composites and will serve for comparison of theoretical predictions such as molecular dynamics models at the very low end and calibration of multi-scale models on higher scales.

Nowadays, **trends in civil engineering** include utilization of various **supplementary components, chemical admixtures, novel particles (e.g. nanoparticles) and recycled or waste materials** used in cementitious or alternative composites. The

behavior of such composites is apriori mostly unknown. With the knowledge of basic building blocks of their microstructure provided by nanoindentation it will become possible to describe their nature without the need of extensive and costly experiments.

So, the work is not at the end. There is still a lot of room for further developments and findings related to nanoindentation. New **rapid indentation** systems are being developed (known as XPM by Hysitron) where hundreds of indents are acquired in a minute. It can be anticipated that this fast technique will allow much faster progress in material characterization, especially for cementitious composites where the size of statistical sets must be large. Combination of advanced experimental techniques of SEM and FIB with nanoindentation will allow to assess other characteristics. Compression **fracture modes and creep** are of prior interests and works are being conducted on FIB prepared samples (micropillars, beams, etc.). Similarly to standard mechanical tools, nanoindentation can also be performed in modes of elevated temperature or in different environments (e.g. variable **humidity or water**). Identification of material characteristics dependent on temperature and humidity are, of course, very attractive for building materials and are worse of further investigations.

11 Acknowledgements

The author would like to thank his wife Jitka for continuous love and support and children Petr and Míša for patience with their daddy.

The author would like to express thanks to all collaborators that substantially attributed to achievements gained on his almost twenty years long track in the nanoindentation endeavor. Particularly Z. Bittnar, V. Šmilauer, J. Zeman, P. Kabele, L. Kopecký, O. Jiroušek (ÚTAM Praha), J. Menčík (University Pardubice), F. Lofaj (SAS Košice), former Ph.D. students K. Forstová, J. Vondřejc and V. Králík. L. Pešek (TU Košice) is acknowledged for his unflagging effort in organizing Local Mechanical Properties symposium and putting national and international researchers in nanoindentation field together. Former and present scientists from Institute of Physics, Czech Academy of Sciences (L. Polívka, J. Bočan, J. Maňák, A. Jäger) are acknowledged for their help with FIB. Prof. Yunping Xi (University of Colorado in Boulder) is acknowledged for joint research directions and for offering an Adjunct Professorship at CU Boulder.

12 References

- [1] J. Němeček, “Creep effects in nanoindentation of hydrated phases of cement pastes,” *Materials Characterization*, vol. 60, pp. 1028–1034, 2009.
- [2] J. Němeček, V. Šmilauer, and L. Kopecký, “Nanoindentation characteristics of alkali-activated aluminosilicate materials,” *Cement and Concrete Composites*, vol. 33, no. 2, pp. 163 – 170, 2011.
- [3] J. Menčík, L. H. He, and J. Němeček, “Characterization of viscoelastic-plastic properties of solid polymers by instrumented indentation,” *Polymer Testing*, vol. 30, no. 1, pp. 101 – 109, 2011.
- [4] J. Němeček, V. Králík, and J. Vondřejc, “Micromechanical analysis of heterogeneous structural materials,” *Cement and Concrete Composites*, vol. 36, no. 0, pp. 85 – 92, 2013.
- [5] W. da Silva, J. Němeček, and P. Štemberk, “Methodology for nanoindentation-assisted prediction of macroscale elastic properties of high performance cementitious composites,” *Cement and Concrete Composites*, vol. 45, pp. 57 – 68, 2014.
- [6] V. Králík and J. Němeček, “Comparison of nanoindentation techniques for local mechanical quantification of aluminium alloy,” *Materials Science and Engineering: A*, vol. 618, pp. 118 – 128, 2014.
- [7] J. Němeček, F. Denk, and P. Zlámal, “Numerical modeling of aluminium foam on two scales,” *Applied Mathematics and Computation*, vol. 267, pp. 506 – 516, 2015. The Fourth European Seminar on Computing (ESCO 2014).
- [8] V. Nežerka, J. Němeček, Z. Slížková, and P. Tesárek, “Investigation of crushed brick-matrix interface in lime-based ancient mortar by microscopy and nanoindentation,” *Cement and Concrete Composites*, vol. 55, pp. 122 – 128, 2015.
- [9] J. Němeček, V. Hrbek, L. Polívka, and A. Jäger, “Combined investigation of low-scale fracture in hydrated cement and metal alloys assessed by nanoindentation and fib,” in *9th International Conference on Fracture Mechanics of Concrete and Concrete Structures FraMCoS-9*, V. Saouma, J. Bolander and E. Landis (Eds), pp. 11–14, 5 2016.

-
- [10] J. Němeček, V. Králík, V. Šmilauer, L. Polívka, and A. J. “Tensile strength of hydrated cement paste phases assessed by micro-bending tests and nanoindentation,” *Cement and Concrete Composites*, vol. 73, pp. 164 – 173, 2016.
- [11] J. Němeček, V. Šmilauer, J. Němeček, F. Kolařík, and J. Maňák, “Fracture properties of cement hydrates determined from microbending tests and multiscale modeling,” in *Computational Modelling of Concrete Structures: Proceedings of the Conference on Computational Modelling of Concrete and Concrete Structures (EURO-C 2018), February 26 - March 1, 2018, Bad Hofgastein, Austria*, Guenther Meschke, Bernhard Pichler, Jan G. Rots (Eds), pp. 113–119, Taylor and Francis Group, London, 2018.
- [12] A. C. Fischer-Cripps, *Nanoindentation*. Springer, 2002.
- [13] M. L. Palacio and B. Bhushan, “Depth-sensing indentation of nanomaterials and nanostructures,” *Materials Characterization*, vol. 78, no. 0, pp. 1 – 20, 2013.
- [14] C. Hu and Z. Li, “A review on the mechanical properties of cement-based materials measured by nanoindentation,” *Construction and Building Materials*, vol. 90, no. 0, pp. 80 – 90, 2015.
- [15] G. Constantinides, K. R. Chandran, F.-J. Ulm, and K. V. Vliet, “Grid indentation analysis of composite microstructure and mechanics: Principles and validation,” *Materials Science and Engineering: A*, vol. 430, no. 12, pp. 189 – 202, 2006.
- [16] F.-J. Ulm, M. Vandamme, M. Bobko, and J. Ortega, “Statistical indentation techniques for hydrated nanocomposites: concrete, bone, and shale,” *Journal American Ceramics Society*, vol. 90, no. 9, pp. 2677 – 2692, 2007.
- [17] L. Gianuzzi and F. Stevie, *Introduction to Focused Ion Beams. Instrumentation, Theory, Techniques and Practice*. Springer, 2005.
- [18] D. E. Armstrong, A. J. Wilkinson, and S. G. Roberts, “Measuring anisotropy in young’s modulus of copper using microcantilever testing,” *Journal of Materials Research*, vol. 24, pp. 3268–3276, 2009.
- [19] J. Gong and A. J. Wilkinson, “Micro-cantilever testing of <a> prismatic slip in commercially pure Ti,” *Philosophical Magazine*, vol. 91, no. 7-9, pp. 1137–1149, 2011.
- [20] V. Šmilauer and Z. Bittnar, “Microstructure-based micromechanical prediction of elastic properties in hydrating cement paste,” *Cement and Concrete Research*, vol. 36, no. 9, pp. 1708 – 1718, 2006.

-
- [21] J. Vorel, V. Šmilauer, and Z. Bittnar, “Multiscale simulations of concrete mechanical tests,” *Journal of Computational and Applied Mathematics*, vol. 236, no. 18, pp. 4882 – 4892, 2012.
- [22] V. Šmilauer, *Multiscale Hierarchical Modeling of Hydrating Concrete*. Saxe-Coburg Publications, 2015.
- [23] M. Hlobil, V. Šmilauer, and G. Chanvillard, “Micromechanical multiscale fracture model for compressive strength of blended cement pastes,” *Cement and Concrete Research*, vol. 83, pp. 188 – 202, 2016.
- [24] P. K. Mehta and P. J. M. Monteiro, *Concrete: Microstructure, Properties, and Materials*. McGraw-Hill, 4 ed., 2014.
- [25] H. M. Jennings, “A model for the microstructure of calcium silicate hydrate in cement paste,” *Cement and Concrete Research*, vol. 30, no. 1, pp. 101 – 116, 2000.
- [26] H. M. Jennings, “Refinements to colloid model of c-s-h in cement: Cm-ii,” *Cement and Concrete Research*, vol. 38, no. 3, pp. 275 – 289, 2008.
- [27] A. J. Allen, J. Thomas, and H. M. Jennings, “Composition and density of nanoscale calciumsilicatehydrate in cement,” *Nature Materials*, vol. 6, pp. 311 – 316, 2007.
- [28] H. Taylor, *Cement Chemistry, Second Edition*. Thomas Telford, 2003.
- [29] J. C. da Silva, P. Trtik, A. Diaz, M. Holler, M. Guizar-Sicairos, J. Raabe, O. Bunk, and A. Menzel, “Mass density and water content of saturated never-dried calcium silicate hydrates,” *Langmuir*, vol. 31, no. 13, pp. 3779–3783, 2015. PMID: 25794183.
- [30] K. L. Scrivener, “Backscattered electron imaging of cementitious microstructures: understanding and quantification,” *Cement and Concrete Composites*, vol. 26, no. 8, pp. 935 – 945, 2004. Scanning electron microscopy of cements and concretes.
- [31] P. Tennis and H. Jennings, “A model for two types of calcium silicate hydrate in the microstructure of portland cement pastes,” *Cement and Concrete Research*, vol. 30, pp. 855–863, 2000.
- [32] G. Constantinides and F.-J. Ulm, “The nanogranular nature of csh,” *Journal of the Mechanics and Physics of Solids*, vol. 55, no. 1, pp. 64 – 90, 2007.

-
- [33] G. Constantinides and F.-J. Ulm, “The effect of two types of c-s-h on the elasticity of cement-based materials: Results from nanoindentation and micromechanical modeling,” *Cement and Concrete Research*, vol. 34, no. 1, pp. 67 – 80, 2004.
- [34] W. Oliver and G. Pharr, “An improved technique for determining hardness and elastic modulus using load and displacement sensing indentation experiments,” *Journal of Materials Research*, vol. 7, pp. 1564–1583, 5 1992.
- [35] Y. Milman, A. Golubenko, and S. Dub, “Indentation size effect in nanohardness,” *Acta Materialia*, vol. 59, no. 20, pp. 7480 – 7487, 2011.
- [36] K. Velez, S. Maximilien, D. Damidot, G. Fantozzi, and F. Sorrentino, “Determination by nanoindentation of elastic modulus and hardness of pure constituents of Portland cement clinker,” *Cement and Concrete Research*, vol. 31, pp. 555–561, 2001.
- [37] A. Zaoui, “Continuum micromechanics: Survey,” *Journal of Engineering Mechanics*, vol. 128, pp. 808–816, 2002.
- [38] H. Moulinec and P. Suquet, “A numerical method for computing the overall response of nonlinear composites with complex microstructure,” *Computer Methods in Applied Mechanics and Engineering*, vol. 157, no. 1, pp. 69 – 94, 1998.
- [39] G. Vainikko, “Fast solvers of the lippmann-schwinger equation,” in *Direct and inverse problems of mathematical physics in international society for analysis. Applications and computation.* (R. P. Gilbert, J. Kajiwara, and Y. S. Xu, eds.), vol. 5, pp. 423 – 440, Dordrecht, The Netherlands: Kluwer Academic Publishers, 2000.
- [40] J. Zeman, J. Vondřejc, J. Novák, and I. Marek, “Accelerating a fft-based solver for numerical homogenization of periodic media by conjugate gradients,” *Journal of Computational Physics*, vol. 229, no. 21, pp. 8065–8071, 2010.
- [41] J. Němeček, V. Králík, and J. Vondřejc, “A two-scale micromechanical model for aluminium foam based on results from nanoindentation,” *Computers and Structures*, vol. 128, no. 0, pp. 136 – 145, 2013.
- [42] V. Koudelková, T. Sajdlová, and J. Němeček, “Micromechanical homogenization of ultra-high performance concrete,” in *Engineering Mechanics 2015*, vol. 821 of *Applied Mechanics and Materials*, pp. 518–525, Trans Tech Publications, 2 2016.

-
- [43] V. Nežerka, J. Zeman, and J. Němeček, “Micromechanics-based simulations of compressive and tensile testing on lime-based mortars,” *Mechanics of Materials*, vol. 105, pp. 49 – 60, 2017.
- [44] V. Zacharda, J. Němeček, and P. Štemberk, “Micromechanical performance of interfacial transition zone in fiber-reinforced cement matrix,” *IOP Conference Series: Materials Science and Engineering*, vol. 246, no. 1, p. 012018, 2017.
- [45] V. Zacharda, P. Štemberk, and J. Němeček, “Nanomechanical performance of interfacial transition zone in fiber reinforced cement matrix,” in *Special Concrete and Composites 2017*, vol. 760 of *Key Engineering Materials*, pp. 251–256, Trans Tech Publications, 2 2018.
- [46] V. Králík, J. Němeček, and P. Koudelka, “Identification of stress-strain relation of aluminium foam cell wall by spherical nanoindentation,” in *Local Mechanical Properties X*, vol. 606 of *Key Engineering Materials*, pp. 11–14, Trans Tech Publications, 6 2014.
- [47] S. A. S. Asif, K. J. Wahl, and R. J. Colton, “Nanoindentation and contact stiffness measurement using force modulation with a capacitive load-displacement transducer,” *Review of Scientific Instruments*, vol. 70, pp. 2408 – 2413, 1999.
- [48] O. Jiroušek, J. Němeček, D. Kytýř, J. Kunecký, P. Zlámal, and T. Doktor, “Nanoindentation of trabecular bone comparison with uniaxial testing of single trabecula,” *CHEMICKE LISTY*, vol. 105, pp. 668 – 671, 2011.
- [49] L. Severa, J. Němeček, v. Nedomová, and J. Buchar, “Determination of micromechanical properties of a hens eggshell by means of nanoindentation,” *Journal of Food Engineering*, vol. 101, no. 2, pp. 146 – 151, 2010.
- [50] Z. Bažant, *Scaling of Structural Strength*. Elsevier Ltd., 2 ed., 2005.
- [51] J. Němeček and J. Němeček, “Microscale tests of cement paste performed with fib and nanoindentation,” in *Special Concrete and Composites 2017*, vol. 760 of *Key Engineering Materials*, pp. 239–244, Trans Tech Publications, 2 2018.
- [52] M. Bauchy, H. Laubie, M. A. Qomi, C. Hoover, F.-J. Ulm, and R.-M. Pellenq, “Fracture toughness of calcium-silicate-hydrate from molecular dynamics simulations,” *Journal of Non-Crystalline Solids*, vol. 419, no. 0, pp. 58–64, 2015.

-
- [53] T. Ghebrab and P. Soroushian, “Mechanical Properties of Hydrated Cement Paste: Development of Structure-property Relationships,” *International Journal of Concrete Structures and Materials*, vol. 4, p. 3743, June 2010.

Resume

11/01/2018

Page 1 of 2

Jiří Němeček**Birth:** 1973. **Nationality:** Czech.**Professional preparation**

1997 **M.Sc.** Czech Technical University in Prague, Civil Engineering Faculty, M.Sc. (Ing.) in Civil Engineering (study branch: Concrete Bridges; graduated with distinction in January 1997).

2000 **Ph.D.** Czech Technical University in Prague, Civil Engineering Faculty, Ph.D. in Structures and Transportation Engineering (dissertation title: "Modeling of Compressive Softening of Concrete"), defended in November 2000, PhD advisor: Prof. Z. Bittnar.

Appointments

2010 – Present **Associate Professor** Czech Technical University in Prague.
 2016/2017 8 months, **Adjunct Professor**, University of Colorado at Boulder
 2013/2014 7 months Fulbright Scholar (senior researcher), University of Colorado (Prof. Y. Xi)
 2000 – 2009 Assistant Professor, Czech Technical University in Prague
 2009 1 month, Visiting researcher, University of Glasgow (Prof. C. Pierce)
 1998, 1999 Visiting scholar, Northwestern University (Prof. Z.P. Bažant)
 1996, 1999 Structural engineer (concrete bridges), Pontex Prague, Ltd. and Sudop Prague.

Research activities and directions

Dr. Němeček primary research interests are in materials characterization (mainly cementitious composites, fly-ash, FRC, HPC, novel metallic structures) using advanced experimental techniques, related microstructure description, multi-scale modeling and applications of novel nano/micro-scale materials and modifications to increase structural integrity and durability. Since 1999, Dr. Němeček has participated in several grant projects as PI or co-PI sponsored mainly by the Czech Science Foundation (CSF), and Ministry of Education and Ministry of Culture of the Czech Republic. Dr. Němeček is an active member of professional organizations, he has organized several international conferences, served as conference proceedings editor and invited editor of a book. He is a member of journal editorial boards. He was invited to give speeches at several international conferences and renowned universities.

Awards

2013-14 Fulbright-Masaryk scholarship

Recent research projects related to cementitious and other composite materials

- Czech Science Foundation (CSF) " Small-scale fracturing of amorphous and crystalline materials assessed with nanoindentation and focused ion beam", 2016-18, PI, budget 7 M CZK.
- Czech Science Foundation (CSF) "Rehabilitation of Reinforced Concrete Structures by Simultaneous Chloride Removal and Nanoparticle Injection", 2016-18, PI, budget 7 M CZK.
- V4-Japan Joint Research Program on Advanced Materials "Multi scale model of the laser dieless drawing process of tubes from hardly deformable magnesium alloys", 2015-18, co-PI budget 389 k€.
- CSF "Determination of Structural and Mechanical Properties of Metal Foams Using Nanoindentation, Computer tomography and Microstructural FEM models", 2012-2014, co-PI, budget 8.7 M CZK.
- CSF "Integration of experimental nanoindentation with numerical tools for upscaling of nanomechanical properties of heterogeneous materials", 2009-2011, PI, budget 3 M CZK.
- CSF "Verification of 3D numerical model for reinforced concrete columns by experimental investigation of effect of lateral reinforcement", 2002-2004, PI, budget 1.5 M CZK.

Professional activities

- Author of over 50 impacted journal papers. Total WoS citations: 551, WoS h-index: 13 (11/2018).

Resume

11/01/2018

Page 2 of 2

- Chair of The World Congress on Civil, Structural, and Environmental Engineering (CSEE'16), March 2016 Prague, Czech Republic | Chair of 5th International Conference on Nanotechnology: Fundamentals and Applications (ICNFA'14), Prague, August 11-13, 2014 | Chair of Nanotechnology in Construction (NICOM3), Prague May 31-June 2, 2009, editor of proceedings (Springer 2009) | Chair of Local Mechanical Properties (LMP), Telč 2009, editor of proceedings.
- Member of scientific committees: NICOM 2009-18 | LMP 2008-17 | 1st International Conference on Nanotechnology in Cement and Concrete CNCC, Irwine, California, 2010
- Member of Editorial Boards: International journal Nanotechnology in Built Environments | Civil-Comp confernecees | Associate editor of International Journal of Theoretical and Applied Nanotechnology.
- Member of professional organizations: international consortium Nanocem | Rilem.
- Founding member of "Center for Nanotechnology in Civil Engineering" (CTU Prague, 2010).
- Author of a book "Nanoindentation in Materials Science" (Intech Publ., 2012).
- Invited lectures: 2017: Special Concretes, CZ; UC Boulder, UCSD California | 2016: Rilem conference, Lyngby, Denmark | 2015: UPC Barcelona | 2014: Gordon Research Conference on Advanced Materials for Sustainable Infrastructure Development, HKUST Hong Kong; University of Colorado; University of Milwaukee; University of San Diego | Nanotexnology 2013, Thessaloniki.
- Supervisor of 5 PhD students (2 current, 3 defended).
- Teaching in undergraduate and graduate courses at Civil Engineering Faculty, CTU Prague

Selected publications

- Němeček, J.; Li, L.; Xi, Y. (2017). Electrokinetic nanoparticle injection for remediating leaks in oil well cement, *Construction and Building Materials* 156, 63-72.
- Němeček, J., Kruis, J., Koudelka, T. et al. (2018). Modeling Simulation of chloride migration in reinforced concrete, *Applied Mathematics and Computation* 319, 575-585.
- Němeček, J., V. Králík, V. Šmilauer, L. Polívka, A. Jager (2016), Tensile strength of hydrated cement paste phases assessed by microbending tests and nanoindentation, *Cement and Concrete Composites* 73, 164-173.
- Němeček, J. (2009). "Creep Effects in Nanoindentation of Hydrated Phases of Cement Pastes", *Materials Characterization*, 60 (9), 1028-1034.
- Němeček, J., Šmilauer, V. and Kopecký, L. (2011). Nanoindentation Characteristics of Alkali-activated Aluminosilicate Materials, *Cement and Concrete Composites*, 33 (2), 163-170.
- Škvára, F., Němeček, J., Kopecký, L. and Bittnar, Z. (2006). "Microstructure of Geopolymer Materials Based on Fly Ash". *Ceramics - Silikáty*, 50 (4), 208-215.
- Menčík, J., He, L.H. and Němeček, J. (2011). "Characterization of viscoelastic-plastic properties of solid polymers by instrumented indentation", *Polymer Testing*, 30 (1), 101-109.
- Šmilauer, V., Hlaváček, P., Škvára, F., Šulc, R., Kopecký, L., et al. (2011). "Micromechanical multiscale model for alkali activation of fly ash and metakaolin", *Journal of Materials Science*, 46 (20), 6545-6555.
- Němeček, J., Králík, V., Vondřejc, J. (2013). "Micromechanical analysis of heterogeneous structural materials", *Cement and Concrete Composites*, 36, 85-92.
- Leal Da Silva, W., Němeček, J. and Štemberk, P. (2014). "Methodology for nanoindentation-assisted prediction of macroscale elastic properties of high performance cementitious composites", *Cement and Concrete Composites*, 45, 57-68.
- Nežerka, V., Němeček, J., Slížková, Z., Tesárek, P. (2015). "Investigation of crushed brick-matrix interface in lime-based ancient mortar by microscopy and nanoindentation". *Cement and Concrete Composites*, 55, 122-128.